Journal Name

Dynamic Article Links ►

Cite this: DOI: 10.1039/c0xx00000x

www.rsc.org/xxxxxx

ARTICLE TYPE

BINOL blocks as accessible triplet state modulators in BODIPY dyes†

Josué Jiménez,[a] Ruth Prieto-Montero,[b] Sergio Serrano,[a] Patrycja Stachelek,[c] Esther Rebollar,[d] Beatriz L. Maroto,[a] Florencio Moreno,[a] Virginia Martinez-Martinez,[b] Robert Pal,[c] Inmaculada García-Moreno,*[,d] and Santiago de la Moya*[,a]

Received (in XXX, XXX) Xth XXXXXXXXX 200X, Accepted Xth XXXXXXXXX 200X
DOI: 10.1039/b000000x

BINOL moieties of different electronic demand are useful blocks for enabling the photo-production and modulation of triplet excited states in readily-accesible BINOL-based *O*-BODIPY dyes from standard *F*-BODIPY precursors. The rapid and rational development of smarter triplet-enabling BODIPY dyes on the basis of this strategy (*e.g.*, TADF biomarker 4a or room temperature phosphor 4g) paves the way for advancing photonic applications based on organic triplet photosensitizers.

Chemical systems efficiently enabling long-lived triplet states upon light absorption (triplet photosensitizers; T-PSs) are pivotal for a plethora of valuable, modern photonic applications beyond conventional photochemistry, from precision medicine to clean energy.[1] For instance, T-PSs with proper, adjusted properties are crucial for advancing cancer photodynamic therapy (PDT),[2] photocatalytic hydrogen production by water splitting,[3] energy conversion by triplet-triplet annihilation (TTA) photon upconversion,[4] organic light emitting diodes (OLEDs) by thermally-activated delayed fluorescence (TADF),[5] or asymmetric photocatalysis,[6] amongst other useful applications.[1]

However, the consecution and modulation of long-lived triplet manifolds is not easy, likely owing to the lack of general guidelines for a workable structural designing.[1c] Indeed, the photo-production of the triplet excited state depends on a proper balance of multiple photophysical phenomena, not only the required light absorption and intersystem crossing (ISC), but also other competitive processes affecting the ISC efficiency, such as fluorescence, phosphorescence, exciton coupling, charge recombination, etc.[1c,d] Moreover, elucidating the mechanism operating in a specific ISC pathway is usually challenging, mainly in organic systems free of heavy atoms,[1a,c,7] complicating the efficient design and development of organic T-PSs with adjusted triplet properties for specific final applications.

During the last years, the BODIPY (boron dipyrromethene) chromophore stands out in the development of T-PSs (*e.g.*, see Fig. 1),[1a,c,2c,7a,b,d,e] the BODIPYs probably being the most investigated organic dyes in this subject, except for the conventional porphyrin derivatives.[1a,c,d] This is mainly due to the straightforward synthesis and easy chemical manipulation of the BODIPY dyes, as well as to the extraordinary sensibility of the BODIPY photophysics to small structural changes.[8] Unfortunately, the development of advanced BODIPY T-PSs commonly involves complex designs of high synthetic demand,[1a,c,d] such as BODIPY-containing heavy-metal complexes (*e.g.*, **1**[9] in Fig. 1), fullerene-involving BODIPYs (*e.g.*, **2**[10] in Fig. 1), or orthogonal BODIPY dimers (*e.g.*, **3**[11] in Fig. 1), amongst others.[1a,c,d] Obviously, such complex designs difficult their easy manipulation to modulate triplet state properties.

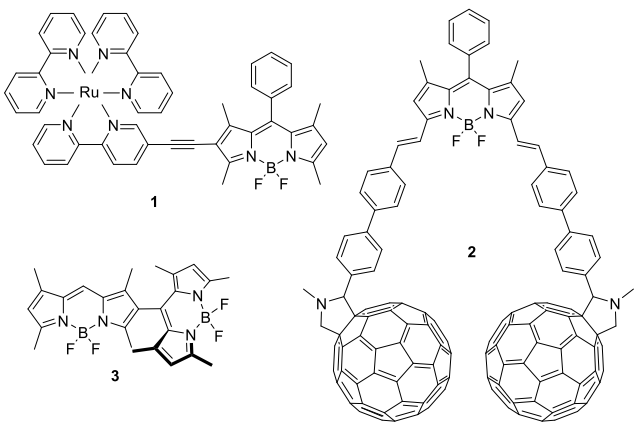

Fig. 1 Examples of BODIPY-based triplet photosensitizers.

In this context, we have recently reported the ability of 3,3´-dibromoBINOL-based *O*-BODIPY **4a** (see Fig. 2) to populate a long-lived triplet state (triplet lifetime >200 μs in deaerated chloroform) by efficient visible-light absorption.[7e] This triplet state population allows the photo-production of singlet oxygen, $^1O_2$, with significant quantum efficiency (ϕ_Δ = 32% in chloroform), while keeping fluorescent ability (ϕ_{flu} = 62% in chloroform), a valuable dual behaviour for photo-theragnostics.[7e] However, related BINOL-*O*-BODIPY **4b** (Fig. 2), involving electron-poor phenyl moieties instead of bromines at the BINOL subunit, gives place to silent production of $^1O_2$ favouring fluorescence (ϕ_Δ = 0%; ϕ_{flu} = 90%). Under the same experimental conditions, **4c** (Fig. 2), involving non-substituted BINOL, enabled photo-induced electron transfer (PET) (ϕ_Δ = 0 %; ϕ_{flu} = 5%).[7e]

The differential ability of BODIPYs **4a-c** to populate the triplet state depends on their capability to populate a proper intramolecular charge transfer (ICT) state, which in turn depends on the electronic demand of both the BINOL and the BODIPY molecular subunits (*i.e.*, due to differential *push-pull*

chromophoric effect).[7e] This interesting dependency, together with the easy synthetic access of the BINOL-*O*-BODIPY dyes,[7e] prompted us to investigate the possible consecution and modulation of triplet states in BODIPY dyes by using the accessible BINOL-*O*-BODIPY design.

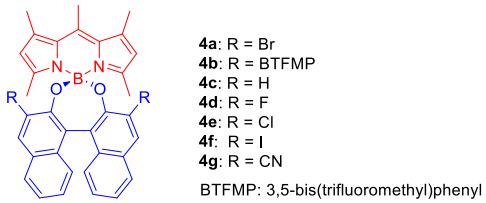

Fig. 2 Selected BINOL-*O*-BODIPY dyes. BINOL and BODIPY subunits in blue and red respectively.

For this purpose, we selected the series **4a-c,d-g** (Fig. 2), which involves BINOL-*O*-BODIPY dyes with the same pentamethylated BODIPY subunit, and BINOL moieties 3,3´-disubstituted with different electron-withdrawing groups (fluoro for **4d**, chloro for **4e**, bromo for **4a**, iodo for **4f**, and cyano for **4g**) or non-substituted at such positions (**4c**), in order to gradually cover an ample palette of electronic effects modulating the BODIPY-chromophore *push-pull* effect. Satisfactorily, new **4d-g** could be straightforwardly synthesized from commercial *F*-BODIPY PM546 (1,3,5,7,8-pentamethyl-*F*-BODIPY) and the corresponding 3,3´-disubstituted BINOL,[12] according to the procedure used previously for **4a-c** (see ESI†).[7e] As expected,[7e] the different electron-withdrawing ability of the new substituents at the BINOL subunit (fluoro, chloro, iodo and cyano) affects both the fluorescence and the photoproduction of $^1O_2$ of **4d-g** when compared to previously studied **4a** and **4b** (Table 1).

Table 1. Singlet-oxygen photo-production quantum yield (ϕ_Δ), fluorescence quantum yield (ϕ_{flu}), and lifetimes of triplet excited states (τ^T) of **4a,c-g** in chloroform. Hammett´s σ_p parameters for the BINOL substituents are included for the comparison of key electronic effects.

Substituent	H	F	Cl	Br	I	CN
σ_p [a]	+0.00	+0.06	+0.23	+0.23	+0.18	+0.66
Dye	**4c** [b]	**4d**	**4e**	**4a** [b]	**4f**	**4g**
ϕ_Δ (%)	0	7	9	32	67	5
ϕ_{flu} (%)	5	67	82	62	12	87
τ^T (μs) [c]	-	-	-	238	119	-

[a]Hammett´s σ_p parameter (ref. 13). [b]Data from ref. 7e. [c]Determined by ns-TA spectroscopy in deaerated chloroform solution.

The PET operating in **4c** must be no longer thermodynamically possible in any other of the selected dyes, providing high fluorescence efficiency in solvents of low polarity (see Table 1 and Table S1 in ESI†), except for **4f**. In this last case, the involved heavy iodine atoms significantly contribute to spin-orbit coupling, efficiently populating the triplet state in detriment of the excited singlet state, which leads to one of the lowest fluorescence efficiencies together with the highest $^1O_2$ photo-production within the studied series (ϕ_{flu} = 0.12 and ϕ_Δ = 0.67, Table 1).

The ICT-mediated photophysics was experimentally supported by the marked decrease of fluorescence efficiency when increasing the solvent polarity for all the selected dyes, except for cyano-substituted **4g** (Table S1 in ESI†), which exhibits an intense fluorescence even in polar-enough solvents such as acetonitrile (see Table 1 and Table S1 in ESI†). This behaviour is driven by the strong electron-withdrawing effect exerted by the cyano groups (the highest in the studied series according to Hammett´s σ_p parameters;[13] see Table 1). Therefore, it is clear that the extent in which the electron-withdrawing ability of the BINOL substituents activates ICT states, in combination with possible heavy-atom effects, rules the differential ability of the studied dyes to populate triplet states, which can be qualitative tackled by comparing ϕ_Δ and ϕ_{flu} values in Table 1 (*i.e.*, singlet-excited-state *vs.* triplet-excited-state action), with the exception of PET-enabling **4c**.

In a first approach, population of long-lived triplet excited states in new **4d-f** was proved by nanosecond-resolved transient absorption (ns-TA) spectroscopy (see ESI† for details). All these dyes show ns-TA profiles upon photo-excitation at 500 nm: A ground-state bleaching-band centred at 500 nm and two transient absorptions at 400-450 nm and 550-700 nm, respectively (*e.g.*, see Fig. 3 for the case of **4f**, and Fig. S1 in ESI†). These profiles are similar to that previously recorded from **4a** under the same conditions,[7e] being characteristic for long-lived excited population in BODIPYs.[14] Only the triplet lifetimes of brominated **4a** and iodinated **4f** could be accurately determined by ns-TA spectroscopy, by monitoring the mono-exponential decay at 430 nm, being the lifetime corresponding to **4f** significantly shorter than that previously determined for **4a** under the same experimental conditions (see τ^T in Table 1). This result seems to confirm that heavy-atom effect promoting ISC is notably induced through the BINOL moiety on the acting BODIPY chromophore. Thus, the strongest ISC enabled by the heaviest iodine atoms grafted to the BINOL moiety in **4f** would also promote the $T_1 \rightarrow S_0$ transition, therefore reducing the corresponding triplet lifetime. On the other hand, these lifetimes are strongly shortened by oxygen (see Table S2 in ESI†), for example decreasing from 119 μs for **4f** in deaerated chloroform, to 0.52 μs in oxygen-saturated chloroform (see Fig. S2 in ESI†), confirming the assignation to a long-lived excited state (*e.g.*, see Fig. 3 for the case of **4f**).

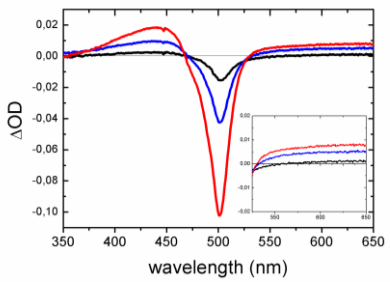

Fig. 3 ns-TA bands of **4f** under nitrogen- (red), air- (blue) and oxygen- (black) saturated chloroform.

More important insights into the exciton-energy transfer promoted in **4a,d-g** are accessible through time-gated spectral analysis of their long-lived emissions induced upon laser excitation at 532 nm in aerated chloroform solutions at room temperature (see ESI† for experimental details).

Heavy-atom free **4d** and **4g** exhibit delayed emission in the 500-650 nm spectral region with similar spectral profile to their prompt laser-induced fluorescence (Fig. 4). The delayed emission intensity increases linearly with the laser pulse energy (Fig. S3 in ESI†), therefore following the expected linear dependence of a one-pho-

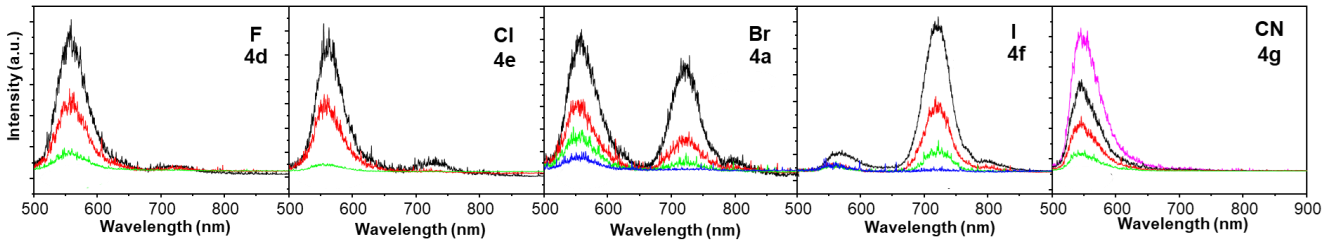

Fig. 4 Delayed emission spectra of **4a,d-g** in chloroform, recorded under ambient conditions upon laser excitation at 532 nm, upon 3 μs (pink), 10 μs (black), 50 μs (red), 100 μs (green) and 200 μs (blue) time delay, respectively. Optically matched solutions were used.

ton process, such as TADF. Considering that prompt fluorescence has lifetimes as short as 6 ns, the remaining delayed emission with lifetimes longer than 100 μs must unequivocally involve long-lived triplet excited states, and emerges through reverse ISC (rISC). In this regard, Density Functional Theory (DFT) calculations performed for both non-substituted and similarly functionalized BODIPYs denoted S_1 and T_2 as nearly isoenergetic excited states sustaining rISC to S_1 as competing decay channel.[15]

As the probability of ISC increases on going from fluorinated **4d** to iodinated **4f**, the spectral profile evolves toward a dual emission, growing a broad long-wavelength band in the 650-800 nm region, specifically peaked at ~720 nm (Fig. 4). The higher the heavy-atom effect on the BINOL moiety and the stronger the induced spin-orbit coupling, the lower becomes the intensity ratio between short-/long-wavelength emission bands. On the basis of the T_1 energy level computed at *ca.* 1.75 eV for *F*-BODIPY PM567 and other related dyes (*O*-BODIPYs),[15] the long-wavelength band recorded at delay times beyond 200 μs (see Fig. 4) can be reliably assigned to the phosphorescence emission. The energy difference between the two lowest excited states (T_1 and S_1) is rather large, that is, ~0.5 eV, as derived from the experimental delayed emission spectra. Hence, this energetic gap should prevent direct population of T_1 from S_1 and *vice versa*, reinforcing the $T_2 \rightarrow S_1$ transition (*i.e*, rISC) as responsible for the delayed fluorescence recorded from **4a,d-g**. Thereby, regarding ns-TA, time-gated emission analysis provides more convincing and unambiguous energetic and dynamic information emerging as a breakthrough spectroscopic strategy.

Additionally, the phosphorescence signatures of **4a** and **4f** (Table S3 in ESI†) could also be determined from the corresponding emission data at 78 K in chloroform (see ESI† for details). The obtained information supports the accurate results obtained by time-gated analysis in the same solvent. Thus, the phosphorescence band appears peaked at 725 nm for both dyes (see Fig. S4 in ESI†), being the phosphorescence quantum yield, ϕ_{pho}, and the phosphorescence lifetime, τ_{pho}, of iodinated **4f** higher and shorter, respectively, than those of brominated **4a** (see Table 1, and Table S3 and Fig. S5 in ESI†), due to enhanced heavy-atom effect (promoting ISC and, therefore, strengthening the $T_1 \rightarrow S_0$ transition) for the former.

Moreover, the determined phosphorescence lifetimes of **4a** and **4f** at 78 K in chloroform (τ_{pho} = 41.9 ms and 7.7 ms, respectively; Table S3 in ESI†) are much longer than those reported from other brominated (within the 2-6 ms interval)[16] and iodinated BODIPYs (<1 ms),[17] respectively, under almost identical conditions, but with heavy halogens directly linked to the BODIPY chromophore instead of linked to pendant moieties. This fact once more indicates a non-conventional ISC operating in these BINOL-*O*-BODIPYs, which is not exclusively promoted by the presence of heavy atoms in the molecular structure.

Interestingly, the possibility of promoting delayed emission by using proper BINOL blocks in BINOL-*O*-BODIPY dyes could serve to rapidly develop advanced bioprobes for useful time-gated microscopy.[18] To investigate this possibility, we selected BINOL-*O*-BODIPY **4a** and **4g**, the former involving the most delayed emission upon laser excitation (see Fig 4), the latter exhibiting the highest fluorescence capability (see Table 1).

Satisfactorily, both dyes were up-taken well by the established mouse fibroblast cell line (NIH 3T3) selected for this study, as supported by using a Laser Scanning Confocal Microscope (LSCM) coupled with an incubator and phase modulation nanoscopy[19] (see ESI† for additional details). As an example, incubation of **4g** (30 μM) in NIH-3T3 cells for 24 hours resulted in uptake of the compound and predominant localization to the lysosomes, as verified by co-localization studies using LysoTracker Red, a well-known red lysosome fluorescent probe (Pearson's correlation coefficient, P = 0.76), and without detecting changes in the cell morphology (see Fig. 5, and Fig S6 in ESI†). These results support the capability of the BINOL-*O*-BODIPYs to act as biocompatible subcellular biomarkers.

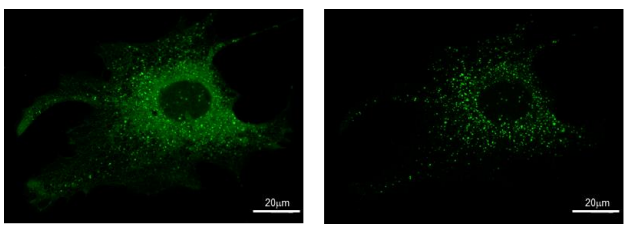

Fig. 5 Bioimaging of a single NIH 3T3 cell by using TADF biomarker **4a**, without (left) and with (right) 1.4 μs time delay.

Interestingly, 3,3´-dibromoBINOL-based **4a** allowed us to record subcellular images by time gated microscopy using a quasi-time delay of 1.4 μs, obtained by scanning between lines at 200 Hz at 1024x1024 pixels. As expected,[18,2b] the obtained time-gated bioimages (lipid droplets; see ESI†) were clearer-cut than those obtained without applying any time delay (see Fig. 5, and Fig. S7 in ESI†), due to confident elimination of the contribution from auto- and background fluorescence. This result evidences the workability of the readily-accessible (commercial) 3,3´-dibromoBINOL block to endow *F*-BODIPY bioprobes with TADF for time-gated microscopy.

In summary, we have demonstrated the capability of accessible BINOL building blocks to promote and modulate triplet states in BINOL-*O*-BODIPY dyes, just by properly selecting the BINOL moiety grafted to the BODIPY subunit. This should allow the rapid design and development of smarter organic T-PSs for advancing a plethora of photonic tools based on long-lived triplet manifolds, such as room temperature phosphors (*e.g.*, **4f**), systems for TTA photon upconversion, TADF-based OLEDs, photocatalysts, etc. Interestingly, biocompatibility, efficient cell up-taken and specific probing, together with easy synthetic access and possibility of designing TADF or/and $^1O_2$ photo-generation, makes the BINOL-*O*-BODIPY design especially valuable to rapidly develop new organic materials with reduced singlet-triplet energy gaps for biomedical applications,[2b] such as TADF biomarkers for time-gated microscopy (*e.g.*, **4a**), or singlet-oxygen photo-generators (*e.g.*, **4a** and **4f**) for advancing both PDT and photo-theragnosis.

Financial support from MICINN (PID2020-114755GB-C32 and C-33, and PID2020-114347RB-C32), Royal Society (URF\R\191002), UE (H2020-MSCA-ITN-859752 and HEL4CHIROLED), BBSRC (BB/S017615/1) and Basque Government (IT912-16) is gratefully acknowledged. J.J., R.P.-M. and P.S. respectively thank CM/UCM, MICINN (MARSA21/71) and BB/S017615/1 for research contracts.

Conflicts of interest

There are no conflicts of interest to declare.

Notes and references

[a] *Departamento de Química Orgánica, Facultad de Ciencias Químicas, Universidad Complutense de Madrid, Ciudad Universitaria s/n, 28040, Madrid, Spain. E-mail: santmoya@ucm.es.*

[b] *Departamento de Química Física, Universidad del País Vasco-EHU, Apartado 644, 48080, Bilbao, Spain.*

[c] *Department of Chemistry, Durham University, Stockton Road, Durham DH1 3LE, Durham, United Kingdom.*

[d] *Departamento de Sistemas de Baja Dimensionalidad, Superficies y Materia Condensada, Instituto de Química Física "Rocasolano", C.S.I.C., Serrano 119, 28006 Madrid, Spain. E-mail: i.garcia-moreno@iqfr.csic.es.*

†Electronic Supplementary Information (ESI) available: Experimental, photophysical and computational details, characterization data and NMR spectra of new compounds. See DOI: 10.1039/b000000x/

1 (*a*) K. Chen, Y. Dong, X. Zhao, M. Imran, G. Tang, J. Zhao and Q. Liu, *Front. Chem.* 2019, **7**, 821; (*b*) X. Cui, J. Zhao, Z. Mohmood and C. Zhang, *Chem. Rec.* 2016, **16**, 173-188; (*c*) J. Zhao, K. Xu, W. Yang, Z. Wang and F. Zhong, *Chem. Soc. Rev.* 2015, **44**, 8904-8939; (*d*) J. Zhao, W. Wu, J. Sun and S. Guo, Song, *Chem. Soc. Rev.* 2013, **42**, 5323-5351; (*e*) H. Xiang, J. Cheng, X. Ma, X. Zhou and J. J. Chruma, *Chem. Soc. Rev.* 2013, **42**, 6128-6185.

2 (*a*) G. K. Couto, F. K. Seixas, Fabiana, B. A. Iglesias and T. Collares, *J. Photochem. Photobiol. B.* 2020, **213**, 112051; (*b*) V.-N. Nguyen, A. Kumar, M.-H. Lee and J. Yoon, *Coord. Chem. Rev.* 2020, **425**, 213545; (*c*) R. Prieto-Montero, A. Prieto-Castaneda, R. Sola-Llano, A. R. Agarrabeitia, D. García-Fresnadillo, I. López-Arbeloa, A. Villanueva, M. J. Ortiz, S. de la Moya and V. Martínez-Martínez, *Photochem. Photobiol.* 2020, 458-477; (*d*) D. Tzeli and I. D. Petsalakis, *J. Chem.* 2019, 6793490.

3 (*a*) S. Cao, L. Piao and X. Chen, *Trends Chem.* 2020, **2**, 57-70; (*b*) J. Zhang, W. Hu, S. Cao and L. Piao, *Nano Res*. 2020, **13**, 2313-2322; (*c*) J. Jayakumar and H.-H. Chou, *ChemCatChem*, 2020, **12**, 689-704.

4 (*a*) L. Huang, E. Kakadiaris, T. Vaneckova, K. Huang, M. Vaculovicova and G. Han, *Biomaterials* 2019, **201**, 77-86; (*b*) X. Guo, Xinyan, Y. Liu, Q. Chen and D. Zhao, Y. Ma, *Adv, Opt. Mat.* 2018, **6**, 1700981; (*c*) N. Yanai and N. Kimizuka, *Acc. Chem. Res.* 2017, **50**, 2487-2495; (*d*) J. Zhou, Q. Liu, W. Feng, Y. Sun and F. Li, *Chem. Soc. Rev.* 2015, **115**, 395-465; (*e*) Y. You and W. Nam, *Chem. Sci.* 2014, **5**, 4123-4135.

5 (*a*) L. Frederic, A. Desmarchelier, L. Favereau and G. Pieters, *Adv. Funct. Mat.* 2021, *31*, 2010281; (*b*) D.-W. Zhang, M. Li and C.-F. Chen, *Chem. Soc. Rev*. 2020, **49**, 1331-1343; (*c*) Y. Im, M. Kim, Y. J. Cho, J. Yong J.-A. Seo, K. S. Yook and J. Y. Lee, *Chem. Mat.* 2017, **29**, 1946-1963; (*d*) Y. Liu, C. Li, Z. Ren, S. Yan and M. R. Bryce, *Nat. Rev. Mat.* 2018, **3**, 18020; (*e*) Y. Tao, K. Yuan, T. Chen, P. Xu, H. Li, R. Chen, C. Zheng, L. Zhang and W. Huang, *Adv. Mat.* 2014, **26**, 7931-7958.

6. T. Rigotti and J. Aleman, *Chem. Commun*., 2020, **56**, 11169-11190.

7 (*a*) Y. Hou, Q. Liu and J. Zhao *Chem. Commun.*, 2020, **56**, 1721-1724; (*b*) Z. Wang, L. Huang, Y. Yan, A. M. El-Zohry, A. Toffoletti, J. Zhao, A. Barbon, B. Dick, O. F. Mohammed and G. Han, *Angew. Chem. Int. Ed.* 2020, **59**, 16114-16121; (*c*) V.-N. Nguyen, Y. Yim, S. Kim, B. Ryu, K. M. K. Swamy, G. Kim, N. Kwon, C,.Y. Kim, S. Park and J. Yoon, *Angew. Chem. Int. Ed.* 2020, **59**, 8957-8962; (*d*) M. A. Filatov, *Org. Biomol. Chem.* 2020, **18**, 10-27; (*e*) J. Jiménez, R. Prieto-Montero, B. L. Maroto, F. Moreno, M. J. Ortiz, A. Oliden-Sánchez, I. López-Arbeloa, V. Martínez-Martínez and S. de la Moya, *Chem. Eur. J.* 2020, **26**, 601-605; (*f*) D. J. Gibbons, A. Farawar, P. Mazzella, S. Leroy-Lhez and R. M. Williams, *Photochem. Photobiol. Sci.*, 2020, **19**, 136-158; (*g*) J. Zhao, K. Chen, Y. Hou, Y. Che, L. Liu, Lang and D. Jia, *Org. Biomol. Chem.* 2018, **16**, 3692-3701.

8 (*a*) Y. Wang, X. Shi, C. Yu, Z. Zhou, L. Gai and H. Lu, *Dyes Pigments*, 2020, **177**, 108275-108279; (*b*) R. G. Clarke and M. J. Hall, *Adv. Heterocycl. Chem.*, 2019, **128**, 181; (*c*) N. Boens, B. Verbelen, M. J. Ortiz, L. Jiao and W. Dehaen, *Coord. Chem. Rev.* 2019, **399**, 213024; (*d*) E. Bodio and C. Goze, *Dyes Pigments*, 2019, **160**, 700-710; (*e*) J. Bañuelos, *Chem. Rec*., 2016, **16**, 335-348; (*f*) N. Boens, B. Verbelen and W. Dehaen, *Eur. J. Org. Chem.*, 2015, 6577-6595; (*g*) G. Ulrich, R. Ziessel and A. Harriman, *Angew. Chem. Int. Ed.*, 2008, **47**, 1184-1201.

9 W. Wu, J. Sun, X. Cui, Y. Chi and J. Zhao, *J. Mater Chem. C*. 2013, **1**, 4577-4589.

10 L. Huang, X. Yu, W. Wu and J. Zhao, *Org. Lett.* 2012, **14**, 2594-2597.

11 Y. Cakmak, S. Kolemen, S. Duman, Y. Dede, Y. Dolen, B. Kilic, Z. Kostereli, L. T. Yildirim, A. L. Dogan, D. Guc and E. U. Akkaya, *Angew. Chem. Int. Ed.* 2011, **50**, 11937-11941.

12 (*a*) T. R. Wu, L. Shen and J. M. Chong, *Org. Lett.* 2004, **6**, 2701-2704; (*b*) H. M. Turner, J. Patel, N. Niljianskul and J. M. Chong *Org. Lett.* 2011, **13**, 5796-5799; (*c*) Y. Zhang, N. Li, B. Qu, S. Ma, H. Lee, N. C. Gonnella, J. Gao, W. Li, Z. Tan, J. T. Reeves, J. Wang, J. C. Lorenz, G. Li, D. C. Reeves, A. Premasiri, N. Grinberg, N. Haddad, B. Z. Lu, J. J. Song and C. H. Senanayake, *Org. Lett.* 2013, **15**, 1710-1713.

13 C. Hansch, A. Leo and R. W. Taft, *Chem. Rev.* 1991, **91**, 165-192.

14 Z. Mahmood, M. Taddei, N. Rehmat, L. Bussotti, S. Doria, Q. Guan, S. Ji, J. Zhao, M. Di Donato, Y. Huo and Y. H. Xing, *J. Phys. Chem. C*, 2020, **124**, 5944-5957.

15 I. Garcia-Moreno, V. Postils, E. Rebollar, M. J. Ortiz, A. R. Agarrabitia and D. Casanova, *Phys. Chem. Chem. Phys.*, 2022, **24**, 5929-5938.

16 X.-F. Zhang, X. Yang, K. Niu and H. Geng, *J. Photochem. Photobio. A* 2014, **285**, 16-20.

17 R. Prieto-Montero, R. Sola-Llano, R. Montero, A. Longarte, T. Arbeloa, I. López-Arbeloa, V. Martínez-Martínez and S. Lacombe, *Phys. Chem. Chem. Phys*., 2019, **21**, 20403-20414.

18 R. Pal, A. C. J. Barker, D. Hummel and L.-O. Pålsson, *J. Fluoresc.*, 2019, **29**, 255-263.

19 R. Pal, *Faraday Discuss*., 2015, **177**, 507-515.

